FINE GRAINED HODOSCOPES BASED ON SCINTILLATING OPTICAL FIBRES

S.R. BORENSTEIN (York College, CUNY, USA)

and

R.C. STRAND (Brookhaven National Laboratory)

Abstract

This is a description of the development and testing of scintillating optical fibers for use in a fine grained hodoscope for experiments in High Energy Physics. After a brief discussion of the need for such a device in experiments in high rate environments, a description is given of the process of drawing and cladding plastic scintillator to form scintillating optical fibers. This is followed by a description of the test procedures used to evaluate the resultant fibers both in the laboratory and at the accelerator. A discussion of three possible readout schemes then follows. These are individual photomultiplier tubes, avalanche photo-diodes and microchannel plates with segmented anodes. The results of this study are then presented. The present status of the project is then summarized, in which it is pointed out that significant improvement in useful fiber length has been achieved as a result of this development program. The difficulty of quality control in fiber production remains a serious limitation, and a satisfactory readout scheme with good optical coupling between many hodoscope elements and photodetectors has yet to be achieved.

INTRODUCTION

Certain experiments in High Energy Physics require at least some detectors to function in very high rate environments. This might arise in regions near the interaction in fixed target machines, when the beam intensity is very high, or near the intersection region in intersecting beam accelerators, when the luminosity is very high. To meet this need the authors embarked in a research and development project to construct a fine grained hodoscope using scintillating fibers as the resolution element. In conjunction with Galileo Optical Corporation The Brookhaven and York College physicists have been producing, studying and testing scintillating fibers which have been drawn from plastic scintillator rods and clad with a suitable material of lower refractive index. Individual fibers have been tested and characterized as to light yield, attenuation length, and mechanical properties. Several preliminary attempts to assemble groups of fibers into prototype hodoscopes have been carried out and the resulting products have been studied. Some thought has been given to the problem of readout of the light pulses coming from hundreds of fibers in such a hodoscope. In particular, we have considered arrays of small diameter photomutiplier tubes. (PMT) arrays of avalanche photo diodes (APD) and segmented anode microchannel plate (MCP) photo-multipliers. These studies have been carried out both in the laboratory with an electron source, as well as at the AGS with a beam of pi mesons. Some of the results of this work have already been reported elsewhere [1].

MOTIVATION and Problem Definition

As one looks for ever more rare events in experiments in High Energy Physics, it becomes necessary to reject an increasing number of uninteresting events before selecting those which are wanted. This means that the detectors which are close to the interaction region must function in very high rate environments and be capable of resol-

ving events which are separated in time by several nanoseconds. At the same time they must provide the overall analysis system with acceptable spatial resolution. Clearly, the definition of acceptable is context dependent. In the present case, it was felt that a goal to strive for was a hodoscope module on the order of 1 m by 1 m in area with a spatial resolution of the order of 1mm.

Early attempts[2] to draw bare scintillating filaments yielded useful lengths on the order of 15 cm. It was concluded[3] that the useful length was limited by the reflection ineffeciency at the plastic to air interface. Consequently it was decided that cladding the fiber with a material of appropriate index of refrection was a crucial step, in which initial light capture is traded off against increased attenuation length. The principle of the scintillating fiber is illustrated in figure 1, where the light produced by the the particle track is collected at either end of the fiber by multiple internal reflections. The hodoscope is then assembled as a bilayer of fibers in which the centers of the fibers in one layer are offset by one radius from those of the next layer. The initial light yield for minimum ionizing particles is directly proportional to the thickness of the fiber. The amount of light captured is dependent on the numerical aperture of the fiber which is determined by the relative indices of refraction of the core and cladding materials. The final amount of light collected depends on the bulk attenuation length of the scintillating core, the reflection efficiency at the core to cladding interface and on the optical coupling between the fiber and the photodetector. It is clear then, that it is desirable to have as efficient as possible a scintillator material with a long attenuation length, a high index of refraction, and a very rapid scintillation pulse. The ideal cladding should have a low index of refraction, should not be lossy as a light transmitter, should bond well to the cladding and should be rugged so as to withstand handling.

The best combination of scintillator speed and efficiency has been obtained with plastic polyvinyl toluene (PVT). Several cladding materials have been tried, such as silicone, acrylic and glass resin. The best results to date have been with the silicone cladding, but a cladding with a lower index of refraction would obviously improve the overall light capture. In summary the problem at hand is to produce long (order of 1m) narrow (order of 1 or 2 mm) scintillating fibers of uniform diameter, in which a solid bond exists between the core and the cladding, and which provides a quantity of light (order of 25 photons) which can be detected with very high efficiency. Since it is desired to make hundreds of such fibers special attention must be paid to the question of quality control.

Fiber Production

Plastic scintillator preform has been obtained from one of several commercial sources, in the form of polished rods about 4 feet in length and one inch in diameter. The rod is then pulled into a fiber by Galileo Electro Optical. The core of the fiber is drawn from a heated preform as shown in figure 2, and an outer cladding is applied in line on the optically smooth surface of the core as it emerges from the oven. As the draw continues, the cladding is cured either by heat or by application of ultraviolet radiation. Tension is applied to the drawn fiber by one of two methods. In one case, referred to as drum draw, the fiber is wrapped around a capstand and then around a take-up reel which supplies the tension. In the other method, referred to as cane draw, the tension is applied via pinch-wheels, and the fibers are cut into canes of appropriate length as they are being drawn.

The disadvantage of the capstan method is that as the fibers are wound on the the take-up reel, they acquire a set corresponding to the diameter of the reel. For 1 mm diameter fibers this is no problem as they can easily be stetched straight after being cut to size. For

larger diameters the set is permanent, and the pinch-wheel cane draw method is used. The disadvantage here is that the pinch-wheel may damage the cladding surface. This can seriously interfere with the proper function of the fiber if the damage extends to the cladding to core interface.

Experimental Setup

Laboratory Measurements

The test apparatus used for evaluating individual fibers in the laboratory is shown schematically in figure 3. The fiber is coupled to the analyzing PMT at one end and is irradiated with electrons from a Ruthenium 106 source, whose distance from the PMT end of the fiber is varied. The fiber is also sandwiched by a pair of triggering scintillating chip counters. The analyzing PMT (referred to as S) has its output sent to a multichannel analyzer operating in the "charge" or integrating mode. The analyzer is gated by a coincidence of the two chip counters (T1 and T2). The performance of the fiber is characterized by the number of photoelectrons delivered to the first stage of the PMT, as well as by the detection efficiency which is defined as: (S.T1.T2)/(T1.T2) These performance parameters are then studied as a function of the distance between the source and the PMT.

The number of photoelectrons delivered is extracted from a study of the spectrum of the pulse area as obtained from the multichannel analyzer. The appearance of this spectrum is generally a very steeply falling pedestal followed, for most PMTs, by a "Gaussian" shaped distribution, the mean value of which is proportional to the number of photoelectrons. In most cases this limits one to a comparison of relative numbers only. In this analysis, the PMT used was the RCA 8850 which, by virtue of a very high gain first dynode, has single photoelectron resolving capability. A set of typical spectra obtained from the 8850 is shown in figure 4, in which it is seen that not only the mean but also the shape of the distribution is a function of the

mean number of photoelectrons. In particular, the distribution is essentially a convolution of an ideal Poisson distribution based on the mean number of photoelectrons, and a pseudo-Gaussian distribution whose width is a function of the statistics of the multiplication factor of the first dynode. Indeed this is the case for all PMTs, but whereas the ordinary first dynode has a gain of about 6, and therefore a statistical accuracy of the order of 40%, the 8850 first dynode has a multiplication factor of about 40, and a statistical accuracy of about 16%. In the former case, the Gaussian totally washes out the valleys between the Poisson peaks, whereas in the latter case the peaks are resolved. In some of the work the tube used was the Hamamatsu 1322, which gave comparable results to the RCA 8850. The EMI 9843 was also used, but whereas it could resolve peak numbers 1 and 2, it could not resolve the higher numbered peaks.

Since the individual photoelectron peaks are resolved, it is possible to calibrate the 8850 spectrum in absolute numbers, totally independent of any variations in the settings of the power supplies, or in the gains of any other associated electronics. Moreover, the authors have established empirically, that whereas a rigorously correct calculation of the mean number is obtained by calculating the moment of the pulse distribution,(a rather tedious process) a very good approximation is obtained by measuring the position of the peak of the distribution, for relatively bright signals (<n> greater than about 5) and by computing the ratio of the heights of the second, third and fourth peaks for weaker signals.

Specifically:

$\langle n \rangle = 3.67h2/h1$	for $\langle n \rangle < 4$
$\langle n \rangle = 4.50h4/h3 - 0.16$	for $3 < \langle n \rangle < 5$
$\langle n \rangle = (x(peak)-x(ped))/(x(1)-x(ped)) + delta$	for $\langle n \rangle > 5$

Where:

<n>	is the mean number of photoelectrons
hi	is the height of the ith peak
x(peak)	is the position of the overall peak of the distribution.
x(ped)	is the position of the pedestal
x(i)	is the position of the ith peak
delta	is an empirical correction factor (order of 0.5)

The efficiency as defined by (S.T1.T2)/(T1.T2) has meaning only in a relative sense. As seen in figure 3, it is possible as a result of Coulomb scattering, for an electron to hit T1, skim S and hit T2, and thus give a false inefficiency indication. Consequently, the efficiency tends towards some upper limit, rather than 100% as the length tends towards 0, and the true efficiency is obtained by dividing by the maximum apparent efficiency. To lend credence as to the reasonableness of this approach, it is pointed out that the signal from S is discriminated just below the single photoelectron level, and it shoul therefore be possible to predict the efficience from the Poisson statistical expectation of getting one or more hits when the mean number of hits is $\langle n \rangle$: prob(one or more) = $1 - \exp(-\langle n \rangle)$. A set of corresponding data points using 1 mm diameter fibers drawn from the Nuclear Enterprises product NE110 under varying conditions of optical coupling shown in figure 5 bears out the above argument. The data points on the efficiency curves are obtained from the coincidence ratios, while the theoretical curves are obtained by applying the Poisson formula to the number of photoelectrons delivered for the different lengths.

An alternative method of measuring the efficiency consists of adding a second PMT to the other end of the fiber S2, and including it in the coincidence trigger. In this case the efficiency does indeed tend towards 100%. This method was used extensively in the AGS measurements. In order to increase the light yield, and apparent attenuation length, a reflecting tape is applied to one end of the fiber, which has been polished, and in this way a light level increase of about 50% has often been achieved.

In all cases, the results are extremely sensitive to the method of optical coupling between the fiber and the analyzing PMT. In the simplest case, the fiber is butted against the PMT window in a dry joint. This gives the worst possible results. An immediate improvement is obtained by applying a dab of optical grease, and the result

is further improved by gluing the fiber to the PMT. The most practical method is to drill a hole in a clear lucite "cookie" and to pass the fiber throught the hole, glue it, and then polish the face of the cookie until the fiber is flush with the cookie surface. This is then grease or glue jointed to the PMT for a reliable efficient and repeatable optical coupling.

AGS Measurements

To compare the reponse of a fiber to pions with the response to electrons, negative pions from the Brookhaven AGS and electrons from Ruthenium 106 were used to excite the same fiber in the same geometry with the same trigger. The upper two fiber spectra shown in figure 6 correspond to the same fiber being irradiated 30 cm from the PMT, in one case by pions, and in the other case by electrons. The results are essentially identical. The third spectrum was obtained from a different fiber, which was glued to the PMT, and irradiated by electrons. The larger number of photoelectrons in this case underscores both the importance of optical coupling, and also the variation in fiber quality from one batch to another.

A pion is a much finer probe than a coulomb scattered electron to meausure the photon yield as a function of distance from the edge of the fiber. A small beam of pions was triggered by the horizontal overlap of two small scintillation counters. One of them was moved with a micrometer screw so that the amount of overlap could be selected. The single fiber was mounted vertically in a light tight compartment, referred to as the tower, that was carried on a moving stage. Stage coordinates were obtained from a precise lead screw with a pitch of 1 mm. Readout was from a handwheel that had 500 divisions. Backlash in the stage coordinate was eliminated with a return spring, and so the fiber could be scanned to a positional accuracy of about 2 microns. In a way analogous to that described for the laboratory measuements, an RCA 8850 was attached to one end of the fiber, and a

Hamamatsu R647-4 was coupled to the other end of the fiber, about 2.5 cm below the point where the pion beam hit the fiber.

The trigger counters were overlapped by 0.3 mm. They were gated by up-stream counters in the beam transport, and by a 1 mm wide downstream counter just after the tower. This last counter eliminated most of the two particle triggers that missed the fiber. Upstream knock-on electrons were suspected as a major cause of these doublets, which would separately hit the two trigger counters, and simulate a passage through the overlap region. The relative efficiency of the fiber at the upper PMT for this trigger was measured, and the results are shown in figure 7, where the efficiency profile is plotted as a function of the position of the stage. This profile is shown for real probe events as well as for accidentals, obtained by opening a gap between the two overlapping counters. The relative efficiency peaks at bout 70%, and is not flat over the width of the fiber. However, when the shape and size of the accidental profile is corrected for, the "real" profile becomes flat in the fiber region, and is consistent with 100% efficiency. From the shape of the profile, the active fiber is calculated as 1.18 $\pm$ 0.04 mm wide, and the probe is calculated as 0.27 $\pm$ 0.04 nn wide. Direct micrometer measurements of these widths are 1.25 and 0.3 mm respectively.

In order to probe selected horizontal apertures within the fiber, the lower PMT was included in the trigger. When the fiber was centered on the probe, the efficiency was 98%. This corresponds to average pulses of 3.9 photoelectrons at the upper PMT (the 8850). This yield is confirmed by the correponding spectrum shown in figure 8(a), which indicates an average pulse of 3.7 photoelectrons. As the fiber is moved away from the center of the probe, the efficiency falls as fewer photoelectrons per trigger are realized. This reduced yield is confirmed by the pulse spectrum shown in figure 8(b), where an average of 3.0 photoelectons are observed. The central 0.6 mm of horizontal aperture is studied this way. The observed efficience, and

pulse spectra profiles, are compatible with light yields that are proportional to the length of the pion trajectory within the fiber. Hence we can calculate the amount of overlap required for a given efficiency in a two layer hodoscope that is constructed from these round fibers.

Results

The testing procedures described above have been applied to a large number of fibers produced by using combinations of the following list of parameters.

Core	Cladding	Draw Method
NE102	Heat Cured	Draw then Dip
NE110	UV Cured	Clad In Line
NE161	Glass Resin	Drum-Draw
ND100	Silicone	Cane-Draw
BC434	Acrylic	Rod and Tube
	Teflon	Draw & Shrink Wrap

Core Materials

Of the listed core materials, for short lengths, NE102 gives the most light, but due to differences in bulk attenuation superior performance is achieved using NE110 for lengths in excess of about 40 cm. Figure 9 shows a direct comparison of these two materials for various lengths, where the crossover point appears to be about 40 cm. NE161 is equivalent to NE110 as to light yield and attenuation length, but is advertised as having better mechanical properties, and a higher softening temperature. BC434 is substantially equivalent to NE110. It is produced by Bicron Corporation, whereas all the NE scintillators were produced by the US subsidiary of Nuclear Enterprises. ND100 has basically the same scintillation and attenuation properties as NE110, and when used in bulk gives the same light output and efficiencies as the NE products. However, we have not been able to draw this material into a fiber successfully. It should be pointed out that a group at Saclay[4] has reported very encouraging results obtained using extruded polystyrene as the core material. At this point, we are working exclusively with BC434.

Cladding Materials

The plastic scintillator, once it has been drawn, must then be clad with a transparent material of lower refractive index, in such a way that the process of cladding does not destroy the fiber, as would be the case for example, with a heat cured cladding, in which the curing temperature is higher than the softening point of the plastic. We have tried heat cured silicone, and heat cured glass resin provided by various manufacturers. We have also tried UV cured acrylic, and silicone/acrylate as liquid cured cladding materials. We have also tried materials which come in the solid state and are clad in the rod and tube mode. So far the best optical results have been obtained using heat cured silicone cladding. The disadvantage of this material is that the resultant fiber is very fragile. It has a tacky feel to it, and deteriorates with handling. Either a method to minimize handling must be devised, or a buffering coat to protect the silicone must be developed. It does not appear to deteriorate with time, provided that it is not handled. In one case, a silicone coated fiber was painted with white Titanium Oxide paint. This was done in the hope that the reflective nature of the paint might increase the light yield, and also that its opacity would provide isolation between adjacent channels in a hodoscope. The paint caused an immediate deterioration of the fiber. The light level was reduced by about 20% within the first hour after application of the paint. However subsequent to that there was no further deterioration, and the paint acted as an effective protective coating, and the quality of the fiber remained stable for at least one year.

The UV cured acrylic claddings do not give a sufficient numerical aperture to make them useful as a fiber cladding. The glass resin, in some cases, gave very good results; almost as good as the silicone claddings. The problem has been one of repeatability and quality control. More recently experiments have been done with the rod and tube method in which a sleeve of solid cladding material acts as a

sheath to the preform, and the rod and tube are pulled together. This requires that both materials have comparable softening temperatures, and/or that the tube be rather thin to start with.

Drawing Method

In our earliest attempts to produce fibers, the preform was drawn to an unclad fiber, which was then dipped in a cladding bath. The resulting fibers had relatively short attenuation lengths which we attribute to surface imperfections occuring as a result of the long exposure of the unclad fiber to the air prior to dipping.

In the "Clad In Line" method, the fiber passes through a conical cladding jig containing the cladding liquid within a foot of the point of emergence from the drawing furnace. Downstream of the cladding jig is a curing section, in which either heat or UV radiation is applied to effect the curing process. Subsequent to the curing region, the fiber is then taken up by the tension producing mechanism.

The tension is applied in one of two methods: In the Drum-Draw, the fiber is wound first around a capstan, then is taken up by a drum, which determines both the speed and tension of the draw. This produces a continuous length of fiber which is later cut to size. In the Cane-Draw, the fiber is picked up by a pair of pinch wheels, which pull the fiber straight down, and it is then cut to length in line with the draw. The Drum-Draw has the advantage that the fiber is not squeezed by pinch wheels as it is in the Cane-Draw, and is therefor less likely to be damaged in the process. The disadvantage is that the fiber tends to acquire a permanent set corresponding to the diameter of the takeup reel. It has been found that for fibers whose diameter is about 1mm the set can be removed, and the fibers can be pulled straight. For larger diameter fibers, the set remains permanent, and the Cane-Draw is preferred. In this method, the cladding is applied as a thicker layer, about 100 microns (as compared to about 10 microns in the Drum-Draw) so as to protect the cladding to core interface.

In the Rod and Tube method, with which we have experimented most recently, the cladding material is supplied in the form of a loosely fitting sleeve, through which the preform is passed. Together they are mounted in the furnace and drawn. This method was undertaken in the hope of forming a more intimate, and durable bond between cladding and core. Several problems still remain to be solved in this method: The close proximity between rod and tube in the furnace prevents the volatilization of gases that are emitted from the core and bubbles are trapped at the interface. Also, a mismatch in the outer diameter of the core and the inner diameter of the clad causes a ridge to be produced in the fiber. We are continuing to experiment with this method, but so far the best results have been obtained with silicone clad BC434.

A summary distribution of yield and attenuation measurments is displayed in fig. 10, where the shaded region corresponds to a range of performance of both the silicone and glass resin coated NE161 fiber. It should be emphasized that the qualit variations observed are much broader than the width of the shaded band which represents only the perfomance of the more successful draws.

We have characterized the quality of the fiber by an attenuation length, L, where:

$$1/L = 1/b + 1/r; \qquad r = D/\ln(p)$$

D is the diameter of the fiber
p is the probability that a photon survives a reflection at the core to cladding surface.
b is the bulk attenuation length of the scintillator.

The results obtained with the combination of NE161 or BC434 core and silicone cladding are consistent with the following values:

$b = 400$ cm.
$p = 0.999344$

An overview of results obtained with various combinations of core cladding and draw method is given in the following table.

TABLE I

Photoelectrons Delivered and Attenuation Length for a 50 cm. Length of Fiber of diameter 2 mm

\ Draw \\\\\\\ Clad,Core \	In-Line, Drum <n> at 50, Lo	In-Line Cane <n> at 50,LO	Rod & Tube <n> at 50,LO
Bare NE110	<3.0, 50	----------	----------
UV-Acrylic,NE110	4.2, 90 cm	----------	----------
Silicone,NE110	10.0, 140	----------	----------
Silicone,NE161	12.0, 180	8.6, 150 cm	----------
Glass Resin,NE161	10.0, 160	----------	----------
Acrylic, BC434	----------	----------	7.0,70
Teflon, BC434	----------	5.4,33	----------

Hodoscope Construction

Four prototype hodoscope modules have been constructed. The first three were assembled by Galileo immediately after the fibers were drawn. The fourth one was assembled at BNL. All hodoscopes use the silicone clad fibers. The first one was made of 1 mm drum-drawn fibers, the second one of 2 mm drum-drawn fibers, and the third one of 2 mm cane-drawn fibers. The fourth one uses 4 mm diameter cane-drawn fibers. numbers 1 and 3 were tested in the laboratory, and number 2 was tested at the AGS. The biggest problem with these hodoscopes was the quality of the optical coupling between fiber and PMT. The diameter mismatch was such that it was not possible to butt all fibers normally to their respective PMTs. Consequently the hodoscope tested at the accelerator operated with an unacceptably low efficiency.

Hodoscope number 4 was designed to optimize the optical coupling and is shown in figure 11. A module consists of 2 layers of 6 fibers per layer, with the fibers in the upper layer being laterally displaced by about one half diameter relative to those in the lower layer. This is done so that the center to center distance between

fibers can be accurately controlled dispite variations in fiber diameter. The spatial resolution is such that a particle can be located as being in a 1.6 mm window, depending upon which fiber or pair of fibers has been hit. This corresponds to an r.m.s. error of about 0.5 mm.

The ribbon formed by the layer of 6 fibers is about 30 mm in width. These fibers are then coupled to 6 Hamamatsu R1635 PMTs of diameter 9 mm by fanning up and down and left and right as shown in the figure. The important thing is that in the direction of the ribbon width, the PMT assemply also occupies about 30 mm, and so modules of 6 can be added in this direction to make the hodoscope as wide as required. At the other end the fiber is glued to an internally threaded brass rod which can be tightened with a screw to apply the tension necessary to keep the fiber straight in the region of sensitivity. The second layer of 6 fibers is dealt with in a similar way but with the location of the PMTs and the tensioning screws being interchanged. A full fledged hodoscope can now be constructed by adding modules of 6 fibers in the direction of the width of the ribbon. This hodoscope has been tested in the lab but not yet at the accelerator.

Readout Method

Three methods of reading out the hodoscope information from the very large number of channels have been contemplated. The most obvious method is to connect an individual PMT to each fiber. This method is both expensive and very difficult to implement in such a way as to obtain good optical coupling. It is practical only for the largest diameter fibers, operated in regions of low magnetic field. Another method is to couple each fiber to an APD. The small size and immumity to the effects of magnetic field makes the APD a desirable readout element for the scintillating fiber. Work done on development of the APD operated in the Geiger mode will be described later. The third readout method considered is the use of the microchannel plate

(MCP) photomultiplier tube with a segmented anode readout. In this method the fibers are bundled together, and coupled to the photocathode of an MCP tube and the spatial information obtained from the segmented anode is used to establishes the identities of the fibers which have been hit. This method cannot be implemented at present because the photon conversion efficiency of an MCP photomultiplier is about half that of a regular PMT. This is primarily due to the measures which are normally adopted to reduce positive ion feedback in the MCP. Usually this involves the placement of a thin metal film between the cathode and the channel plate. We did perform some measurements with an MCP tube loaned to us by Hamamatsu, but the light yield for a 50 cm long 1 mm diameter fiber was less than 2 photoelectrons. Some manufacturers have been experimenting with non-axial electric fields in the MCP, which would enable them to eliminate the metal film, and presumably to achieve a higher efficiency of photoconversion [5]. At present it might be feasible to use an MCP tube if a proximity focused image intensifier with a fast phosphor were placed between the fiber bundle and the MCP amplifier.

In addition to the three methods of readout already described for general purpose hodoscopes, another possibility exists, when the device is operated in an environment of high intensity but of relatively low multiplicity. This would be the case for example in the case of a beam hodoscope. In this instance considerable economy in readout electronics could by achieved by the use of optical encoding. In a layer containing n elements, the fibers could be grouped in bundles of size square root of n at each end. The grouping would be such that no pair of fibers share the same bundle more than once. In this way for example a 900 element hodoscope could be read out with 60 PMTs. This would work for a beam hodoscope where one hit per event is expected. Slightly higher multiplicities could also be accomodated by making use of the billayer nature of the hodoscope, and extending the encoding concept to the second layer.

Avalanche Photodiodes

As already indicated, the small size and immunity to magnetic field make the APD the photodector of choice. In order to minimize the dark current the silicon APD is cooled to about -70 degrees C, and biased beyond its breakdown voltage so that it operates in the Geiger mode. In this mode which is more sensitive than the avalanche mode a single photoelectron has a probability of initiating a breakdown pulse in the silicon chip, which is a function of the overvoltage. The overall probability of a Geiger pulse is thus a function both of the overvoltage and the number of photoelectrons produced in the silicon. The height of the Geiger pulse is a function only of the overvoltage and therefore contains no analog information.

For our tests, APDs were purchased from RCA. Their entrance apertures are 1.3 mm. They were optimized by RCA for the Geiger mode. A half megohm quench resistor is attached 2 cm from the anode inside a cold fixture where the temperatur is maintained at -70. The external load is a two kilo-ohm resistor. The positive bias is applied to the cathode. The RC recovery time of passive quenching is about 1 micro-second. This imposes a corresponding rate limitation on one channel. To decrease this recovery time would require active quenching [6].

Three methods of coupling the fiber to the silicon chip have been tried. The exit numerical aperture of the fiber is about 0.34 after one attenuation length. This corresponds to an exit half-cone of 20 degrees as shown in (a) of figure 12. In this case the fiber is butted against the window of the APD as it is packaged by the manufacturer in a TO-18 can. About 6% of the light from the fiber falls on the chip. The irregularities of the standard window contribute to further light loss. In figure (b) the window incorporates a lens which enables about 9% of the light to be captured. The glass cone in (c) performed the best. At the thick end it is grease jointed to the fiber, and at the thin end it is cemented to the APD with "crazy glue". Both these

couplings are at low temperatur. In this case, about 40% of the light from the fiber is transmitted to the exit aperture of the cone.

The other end of the fiber is coupled to a PMT. A small counter behind the fiber in coincidence with the PMT provides the triggering for penetration of the fiber by an electron from the Ruthenium source located outside the cold fixture about 50 cm from the APD.

At the breakdown voltage of 368 volts the detection efficiency is zero as shown by the data plotted in figure 13. As the voltage is increased to 400 volts the detection efficiency increases up to a maximum of about 80%. The stability of the setup was confirmed when the maximum efficiency was repeated seven months later. The Ruthenium source was moved 15 cm closer to the APD and the efficiency improved appropriately for an attenuation length of 1.5 m. This efficiency is plotted as an open circle in figure 13. Accidentals to account for the 20% inefficiency are not possible.

The 80% maximum efficiency is consistent with an average number of 50 photons being delivered to the light cone, followed by a coupling efficiency of 0.4, and APD quantum efficiency of 0.8, and an APD triggering probability per photoelectron of 0.2. The figure of 50 photoelectrons is obtained from measurements of an average of 8.6 photoelectrons delivered by a 50 cm fiber to a PMT whose cathode efficiency is 0.17.

If the number of photoelectrons were doubled, by a combination of improved optical coupling, and the use of an antireflection coating on the silicon optimized for the 440 nm scintillator light, the limiting efficiency would become 96%.

Applications

As pointed out in the introduction, this work was motivated by a perceived need for a fine resolution detector to operate at very high rates. The outstanding feature of the scintillating fiber is its ability to deliver a light pulse with a rise time of the order of one

nanosecond. During the course of this research several experimenters in the field of high energy physics have indicated a need for such a device and a desire to incorporate the fibers we have developed in planned experiments. In one case, Leif Jonsson of Lund University has borrowed some of the fibers to study their use in a multiplicity counter in an experiment at DESY. Another possible application is in an experiment recently proposed at the AGS for a Time Separated Anti-proton Beam[7]. Still another experiment (no. 787) at the AGS plans to use a bundle of 4 mm fibers as an active target in a K-meson decay experiment.

Conclusion

We have shown that by drawing and cladding plastic scintillator material it is possible to create thin scintillating fibers with useful lengths in excess of 50 cm. These fibers can then be assembled into fine grained hodoscopes to detect particles in experiments where the rates are such as to exceed the time resolution of the more conventional wire chambers. This represents a significant step forward as compared with the lengths of thin scintillating filaments which have been produced in the past by extruding or by drawing bare plastic. The crucial step is the application of the cladding material in line with the drawing process.

For minimum ionizing particles the amount of light created by the passage of the particle through the scintillator is proportional to the thickness of material, and this clearly places a lower limit to the diameter one can use and still hope to obtain an efficient long fiber. For 2 mm diameter fibers, the data of Table I indicates that one could construct fibers of the order of 1 meter long and still retain enought photons to ensure efficient operation. This results in a resolution cell of 1 mm, or an rms error of the order of 300 microns.

Although we have produced samples of efficient fibers, a number of problems still remain. The most serious problem is the fragility of the final product. The combination with the best optical results has been the silicone clad BC434. The bond between core and cladding appears to be less than intimate, and as a result the quality of the fiber deteriorates with handling, and more seriously, the quality varies from one draw to another. The problem of readout of optical information of a hodoscope with a large number of elements still awaits a satisfactory solution. The direct coupling to PMTs, while feasible, is extremely cumbersome. The use of APDs which would be very attractive is still limited by the photon budget associated with these devices. Another possible mechanism, the use of MCP tubes with segmented anodes, is also presently excluded on the basis of light levels, but further developments in the MCP itself may yield more optically efficient detectors in the future.

Acknowledgments

The author wishes to express his gratitude to colleagues at Brookhaven National Laboratory, without whose help this work could not have been done. First of all my principal collaborator Richard C. Strand, who has co-authored all publications in connection with this work, has always been a pleasure to work with. Special thanks are due to the technical staff of the Lab, and in particular to Edward Frantz and to Joe Scheliga. Finally, I would like to thank Robert Palmer who was instrumental in starting this work, and Howard Gordon, and Tom Ludlam who have supported this project over the last several years.

References

1. S.R. Borenstein and R.C. Strand, "Progress in the Development of Scintillating Optical Fibers", IEEE Transactions on Nuclear Science, NS-31 No. 1, pp 396-398 February 1984.

   S. R. Borenstein and R.C. Strand, "Fine Grained Hodoscopes Based on Scintillating Optical Fibers" Proceedings of 1981 ISABELLE Summer Workshop, BNL 51443, Vol. IV, pp. 1438-1449.

   S.R. Borenstein and R.C. Strand, "Scintillating Optical Fibers" IEEE Transactions on Nuclear Science, NS-29 No. 1, pp. 402-404, Feb. 1982.

   S.R. Borenstein, R.B. Palmer and R.C. Strand, "A Fine Grained Scintillating Optical Fiber Hodoscope for Use at ISABELLE", IEEE Transactions on Nuclear Science, NS-28 No. 1, pp. 458-460, Feb. 1981.

   S.R. Borenstein, R.B. Palmer, and R.C. Strand, "Optical Fibers and Avalanche Photodiodes for Scintillator Counters", presented at the International Conference on Experimentation at LEP, Uppsala, Sweden, 16-20 June, 1980: Physica Scripta, vol. 23, No. 4:1, April, 1981, pp. 550-555.

2. G.T. Reynolds and P.E. Condon, Rev. Sci. Instr., Vol. 28, No. 12, Deceber 1957; G.T. Reynolds, Nucleonics, vol. 16, NO. 6, June 1958.

3. L. Reiffel and N.S. Kapany, Rev. Scie. Instr., Vol. 31, pp. 1136-1142, 1960.

4. L.R. Allemand et al., "Optical Scintillating Fibres for Particle detectors", Proceedings, second Pisa Meeting on Advanced Detectors. (1983)

5. C. Tosswill of Galileo Electro-Optical: Private Communication.

6. S. Cova, A. Longoni and G. Ripamonti, IEEE Transactions on Nuclear Science, NS-29, 599, 1982.

7. AGS Proposal P792 "Development of a Time Purified/Separated Anti-proton Beam and High Precision Cross Section Measurements.

FIGURE CAPTIONS

Fig. 1. a) Scintillating Optical Fiber, Principle of operation;
b) Bilayer of fibersm encapsulated in isolating matrix.

Fig. 2. Plastic Scintillator being Drawn in Furnace.

Fig. 3. a) Schematic of Apparatus for analyzing charge spectrum of scintillating fibers. T1 and T2 define a coincidence telescope. S is the signal to be analyzed.
b) Detail of apparatus showing electron trajectories. Both scattering and counter misalignment have been exaggerated for purpose of illustration.

Fig. 4. Charge Spectra of RCA 8850 PMT excited by low levels of scintillator light.

Fig. 5. Attenuation Curves for 1 mm diameter NE110 fiber:
a) Absolute no. of photoelectrons vs. distance.
b) Efficiency as a function of distance.

Fig. 6. Comparative charge spectra for 30 cm of a 1 mm NE110 fiber that was coupled to a PMT with optical grease and exposed to: (a) 3 GeV/c negative pions; (b) 3.5 Mev betas from 106Ru. (c) is the charge spectrum of a different but comparable 30 cm long fiber that was coupled to a PMT with glue and exposed to 3.5 Mev electrons.

Fig. 7. Efficiency profile of a 30 cm length of 1 mm NE110 fiber in a 3 GeV/c pion beam scanned with a 0.3 mm probe. The solid dots and the trapezoidal curve correspond to real triggers, while the open circles correspond to accidentals.

Fig. 8. Charge spectra for a 30 cm long NE110 fiber in a 3 GeV/c pion beam and a 0.3 cm probe. The upper spectrum is for the probe centered on the fiber, and the lower one is with the probe positioed at the edge of the fiber.

Fig. 9. Direct Comparison of Spectra of NE102 and NE110 fibers using the RCA 8850 PMT.

Fig. 10. Summary attenuation curves for various fibers. Shaded region represents band within many samples of silicone or glass resin coated NE161 fibers fell. In general, the silicone fibers performed near the top of the band, while the glass resin fibers were in the bottom.

Fig. 11. Hodoscope module assembly showing connections to PMTs at one end and to tension screws at the other end. Upper 6 fibers of a 12 fiber bilayer module are shown.

Fig. 12. Three optical coupling arrangements between fiber and APD.
a) Fiber is butted against window of TO-18 can in which the APD is normally packaged.
b) The packaging is modified so that the entrance window is a lens.
c) The fiber is grease jointed to the thick end of a light cone, which has the APD glued to it on the other side.

Fig. 13. APD detection efficiency for a 40 cm length of 2 mm diameter scintillating fiber excited by 3 MeV electrons. The efficiency is plotted as a function of the APD voltage, and is non-zero only above the breakdown voltage. The open circle corresponds to excitation of the same fiber 15 cm closer to the APD.

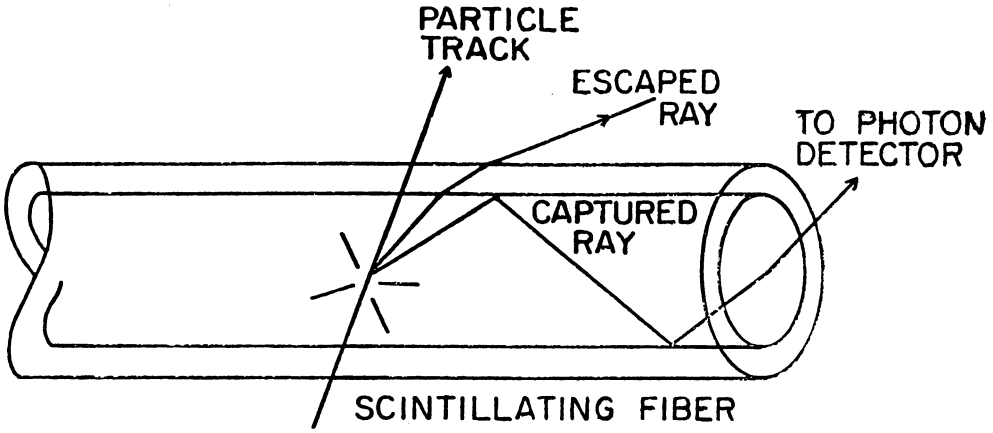
PARTICLE
TRACK
ESCAPED
RAY
TO PHOTON
DETECTOR
CAPTURED
RAY
SCINTILLATING FIBER

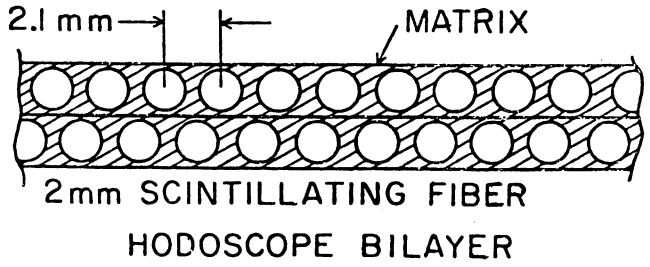
2.1 mm
MATRIX
2mm SCINTILLATING FIBER
HODOSCOPE BILAYER

Fig. 1

DRAWING A
SCINT. FIBRE

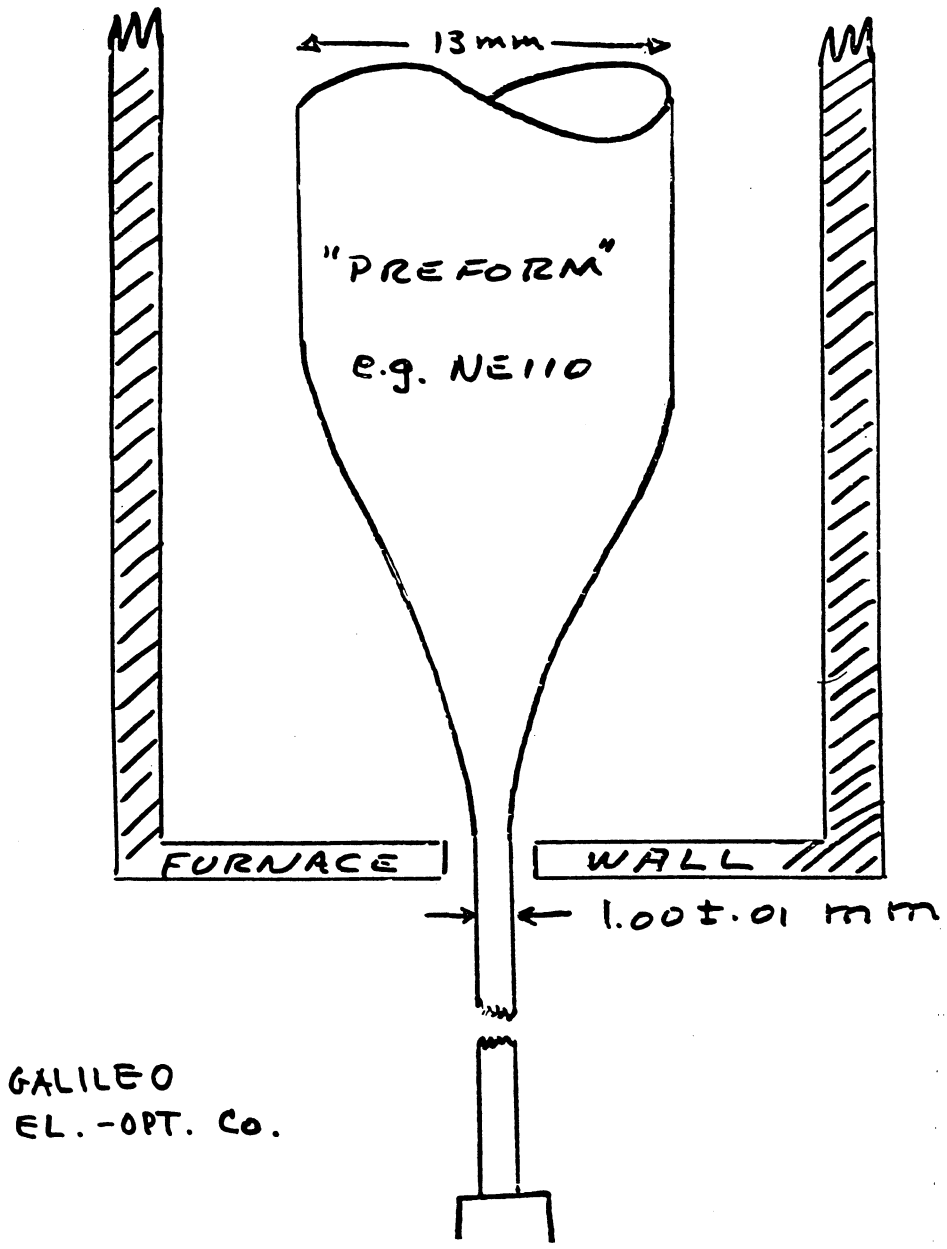

GALILEO
EL.-OPT. Co.

Fig. 2

APPARATUS FOR ANALYZING PULSE HEIGHT SPECTRUM
OF SCINTILLATING FIBER

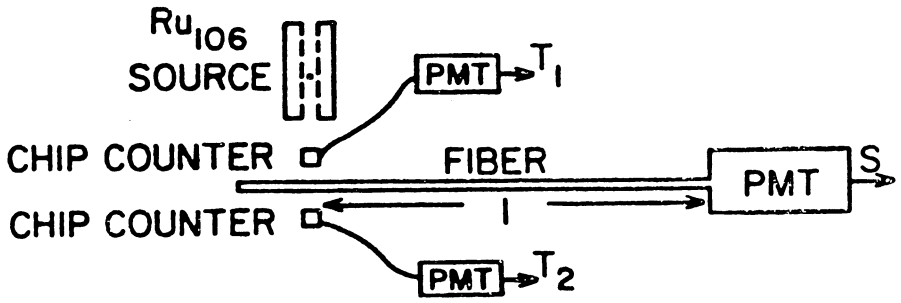

(a) SCHEMATIC

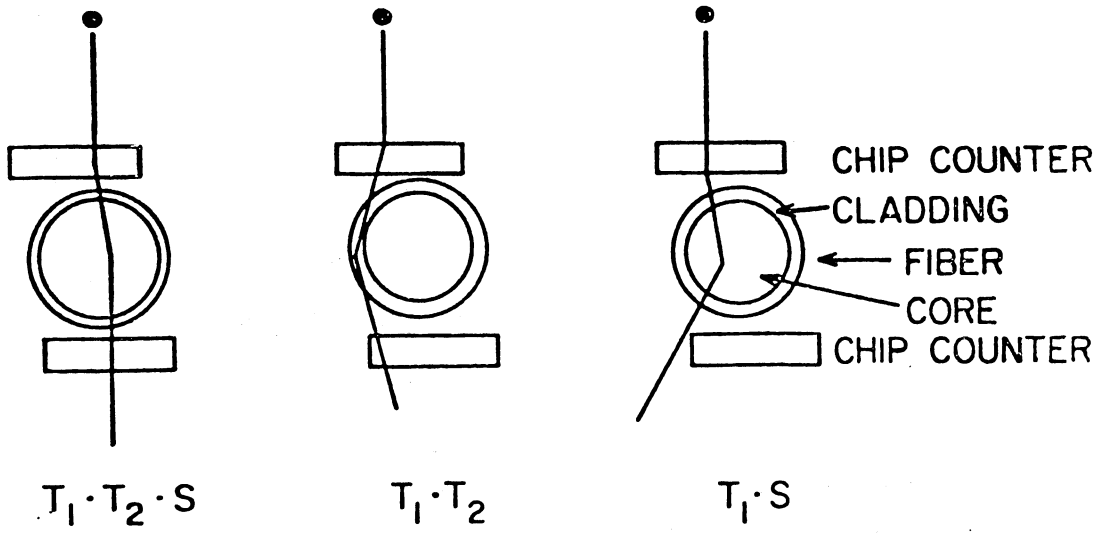

(b) CLOSE UP VIEW OF ELECTRON TRAJECTORY

Fig. 3

CHARGE SPECTRA RCA 8850
EXCITED BY LOW LEVELS OF SCINTILLATOR LIGHT

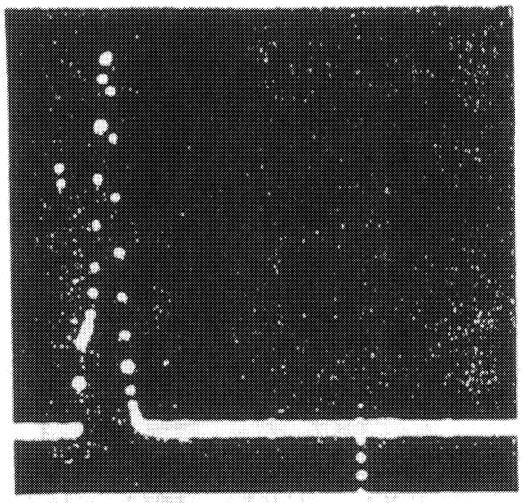

DARK COUNT $\langle n \rangle = 0$
(ESTABLISHES POSITION OF FIRST PEAK)

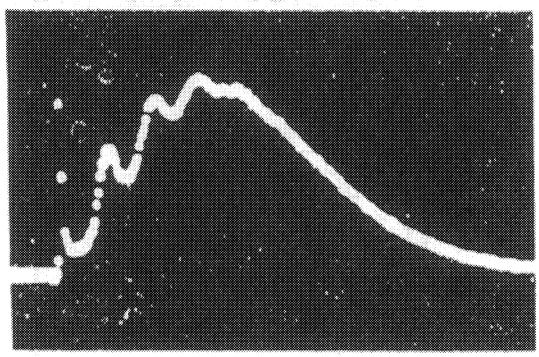

$\langle n \rangle \sim 4$
OBTAINED FROM RATIO OF HEIGHTS OF THIRD AND FOURTH PEAKS

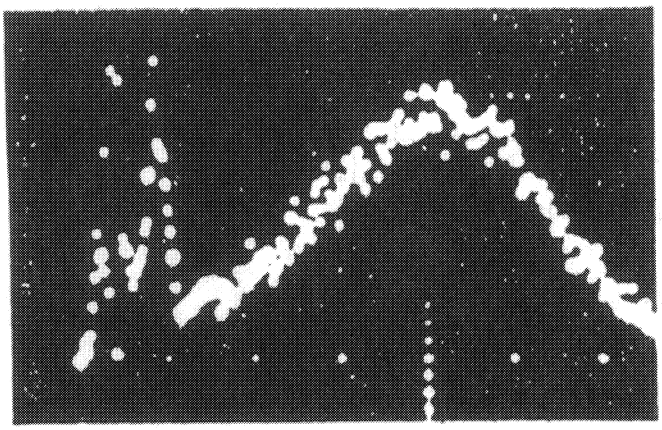

$\langle n \rangle \sim 10$
OBTAINED FROM POSITION OF MAIN PEAK COMPARED WITH THAT OF FIRST PEAK, EACH WITH RESPECT TO PEDESTAL

Fig. 4

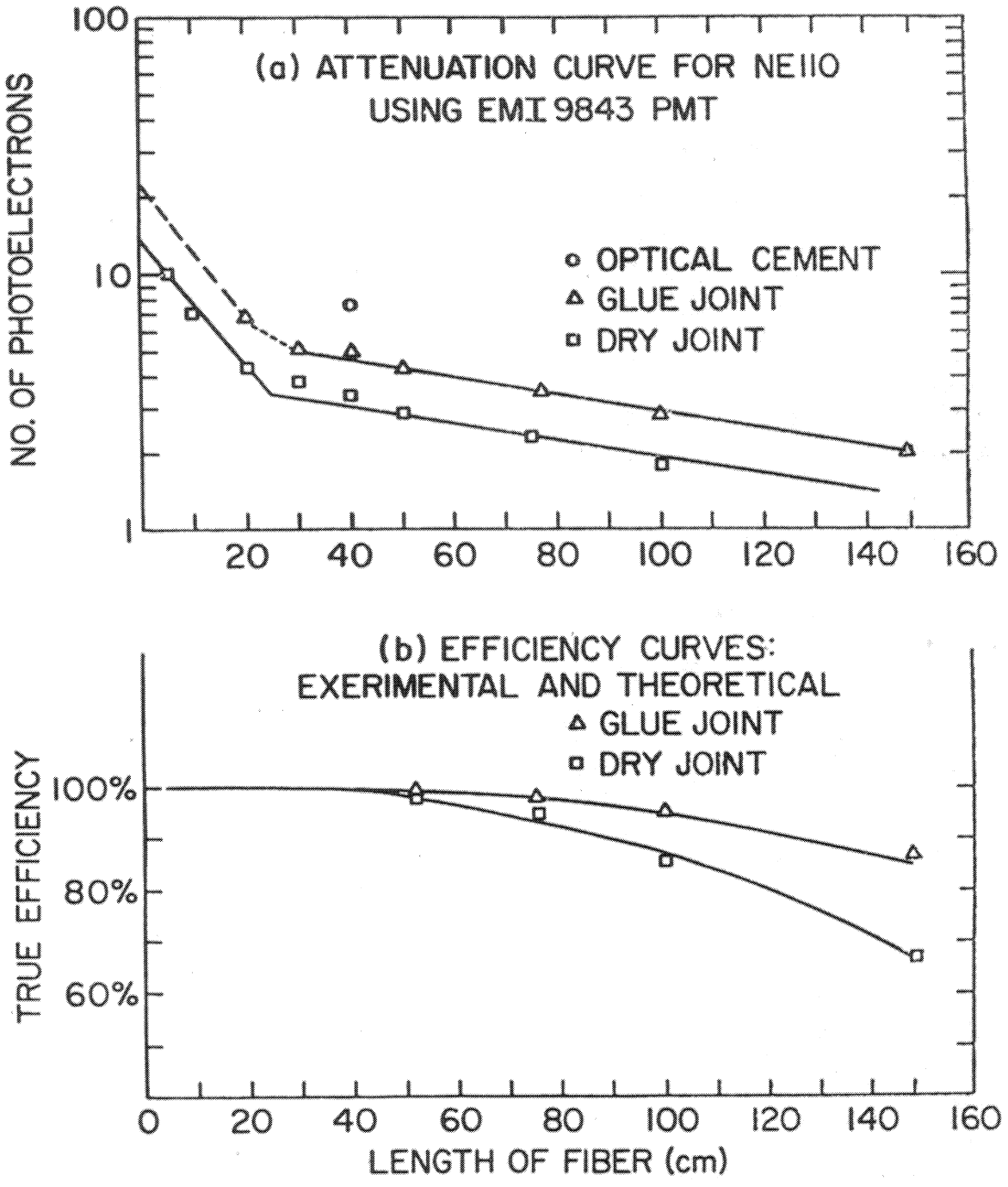
(a) ATTENUATION CURVE FOR NE110
USING EMI 9843 PMT
NO. OF PHOTOELECTRONS
100
10
1
OPTICAL CEMENT
GLUE JOINT
DRY JOINT
20
40
60
80
100
120
140
160
(b) EFFICIENCY CURVES:
EXERIMENTAL AND THEORETICAL
GLUE JOINT
DRY JOINT
TRUE EFFICIENCY
100%
80%
60%
0
20
40
60
80
100
120
140
160
LENGTH OF FIBER (cm)

Fig. 5

FIBER AND BEAM COMPARISONS FOR 30cm LENGTH

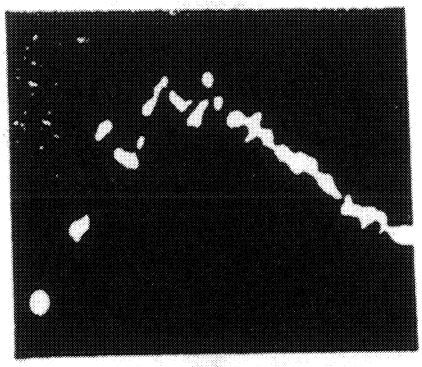

FIBER EXPOSED TO π BEAM
GREASE JOINT TO PMT

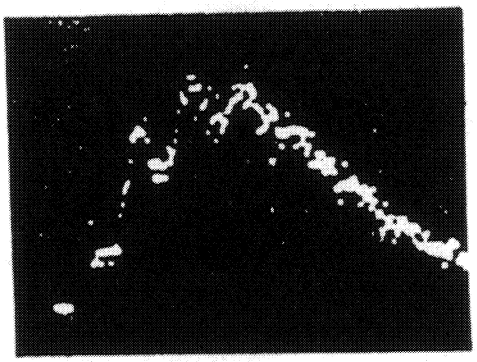

SAME FIBER EXPOSED TO ELECTRONS
UNDER IDENTICAL CONDITIONS

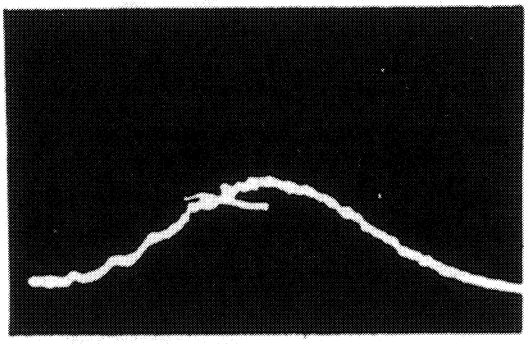

DIFFERENT FIBER EXPOSED TO ELECTRONS
GLUED TO PMT

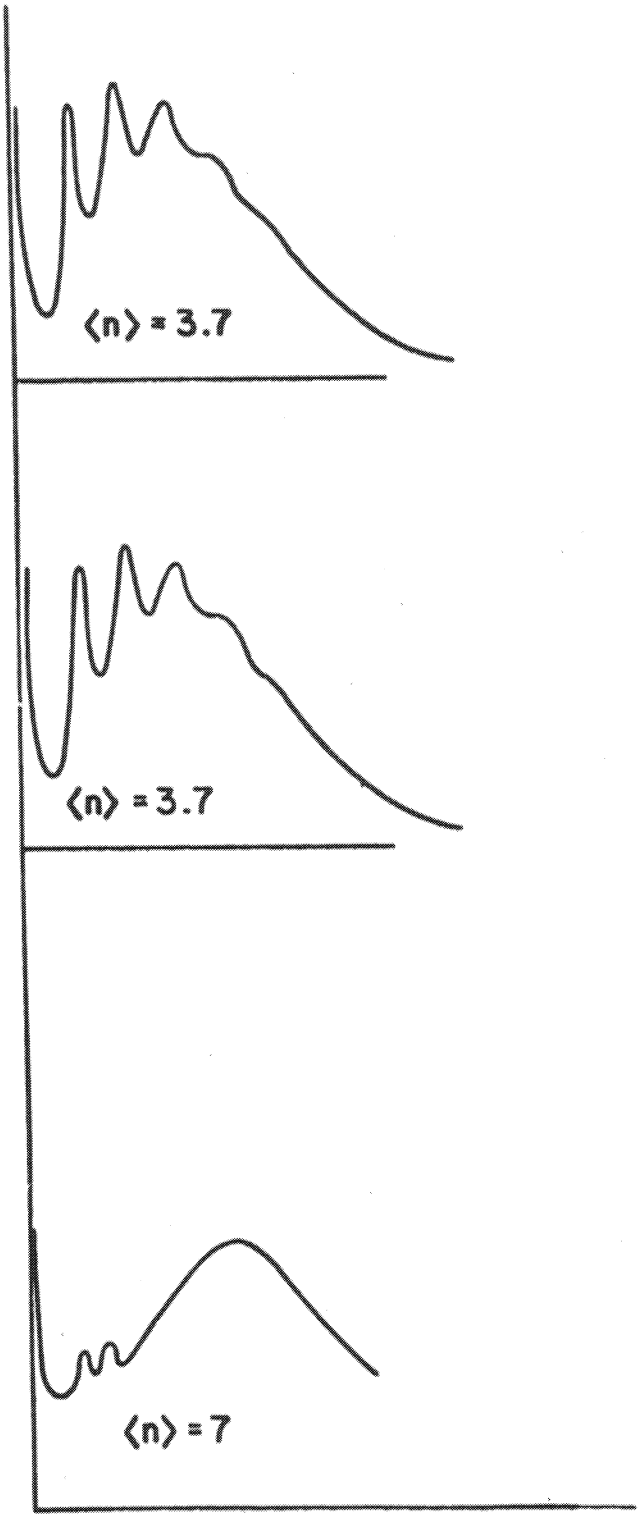

Fig. 6

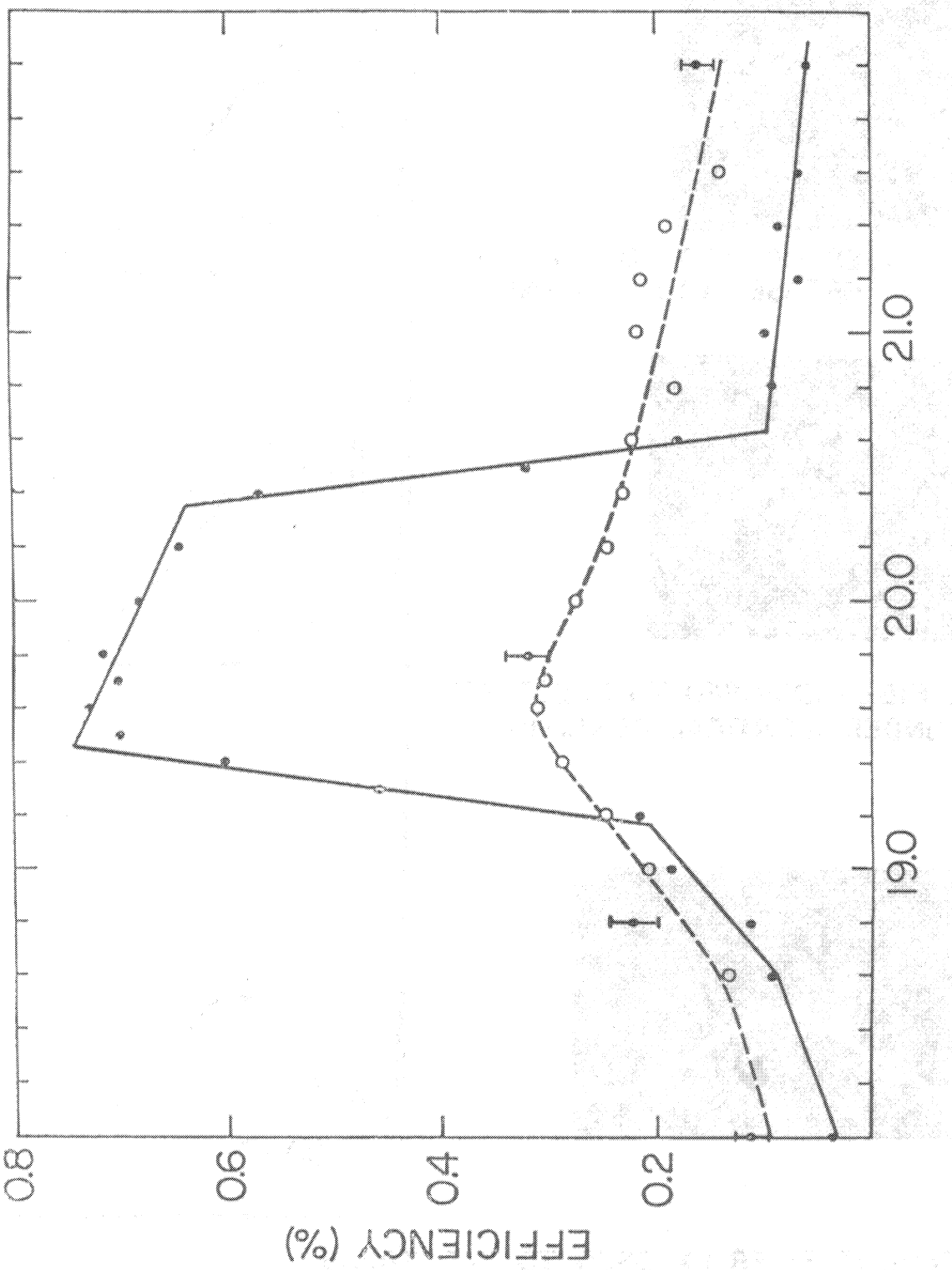

Fig. 7

SIGNAL = S1 GATE = $T_1 \cdot T_2 \cdot \bar{S}_2 \cdot$ BEAM

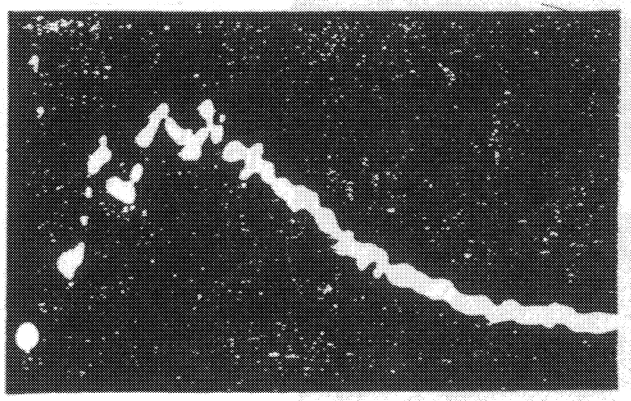

CENTER OF FIBER

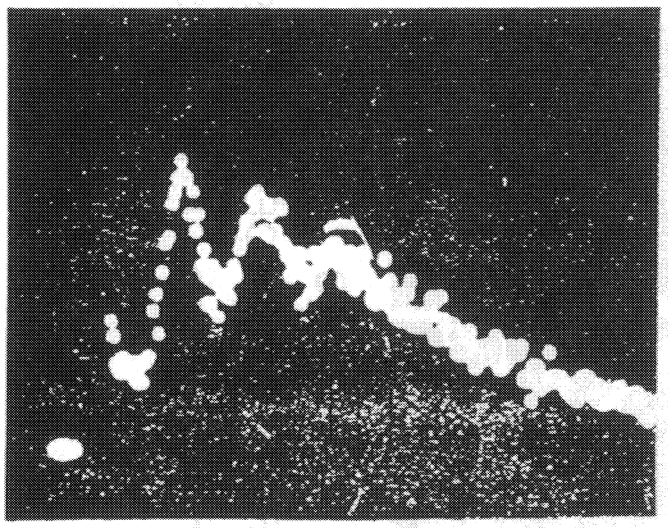

EDGE OF FIBER

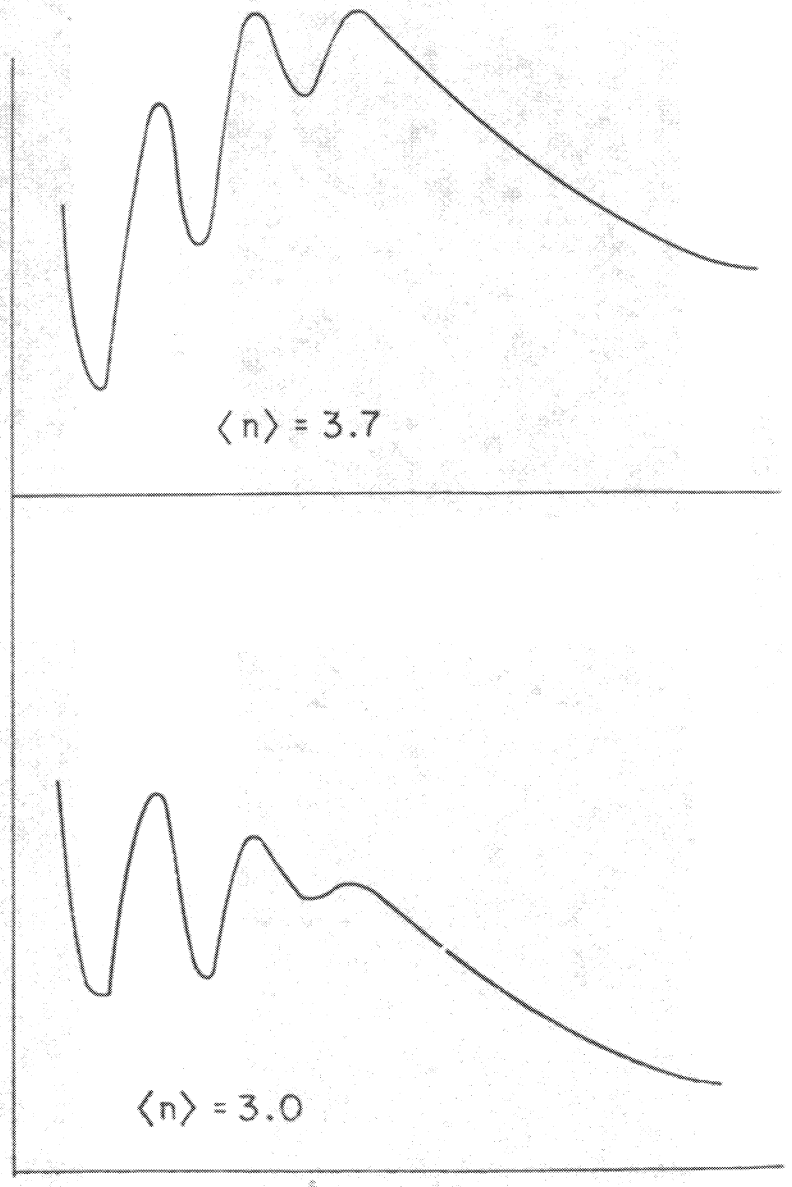

Fig. 8

DIRECT COMPARISON OF NE102 AND NE110 USING RCA 8850

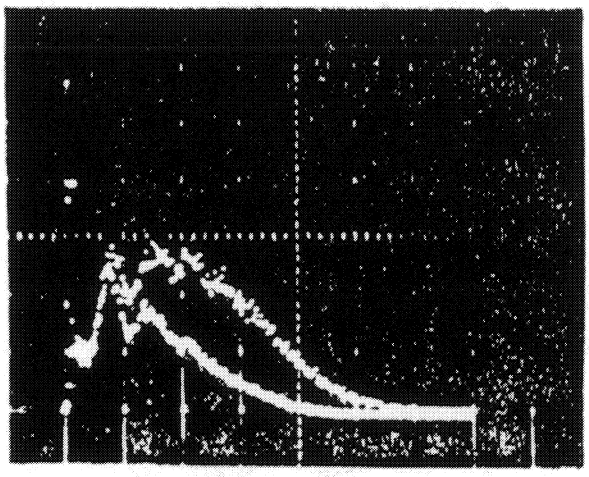

(a) $\ell = 95$

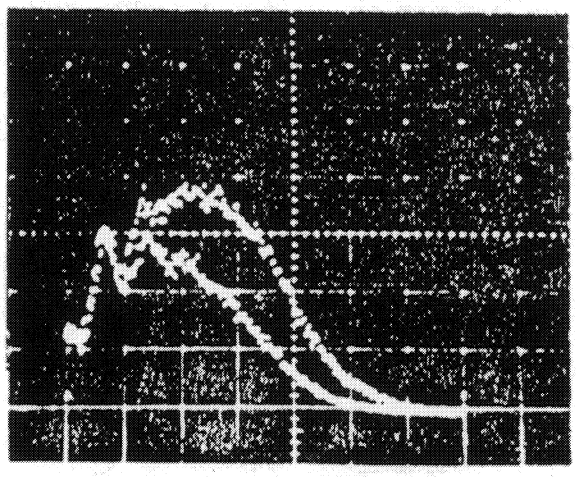

(b) $\ell = 75$

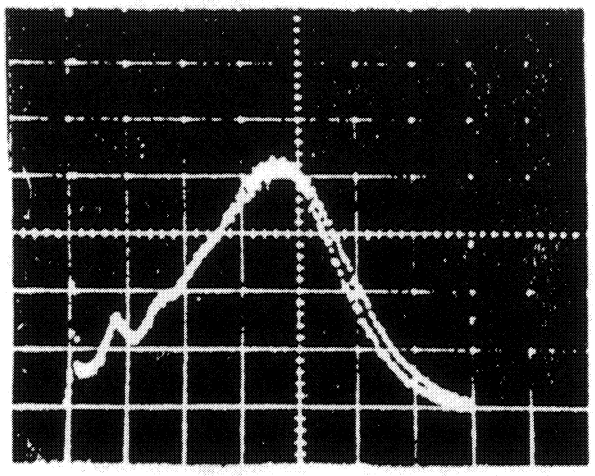

(c) $\ell = 40$

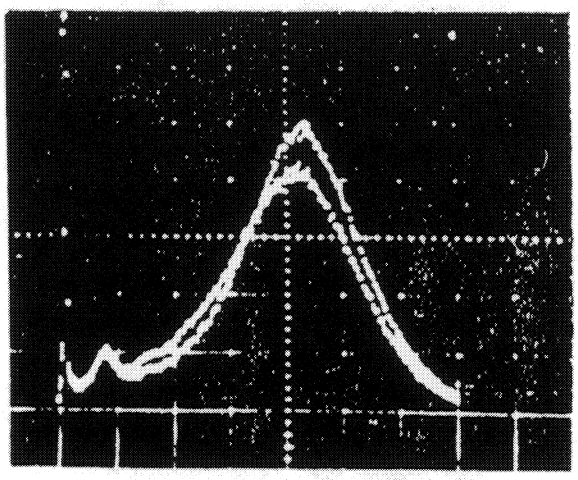

(d) $\ell = 25$

FOR $\ell < 40$, <n> OF NE102 IS HIGHER THAN <n> OF NE110

FOR $\ell > 40$, <n> OF NE110 IS HIGHER THAN <n> OF NE102

Fig. 9

ATTENUATION CURVES FOR
1 mm diam. SCINTILLATING FIBERS

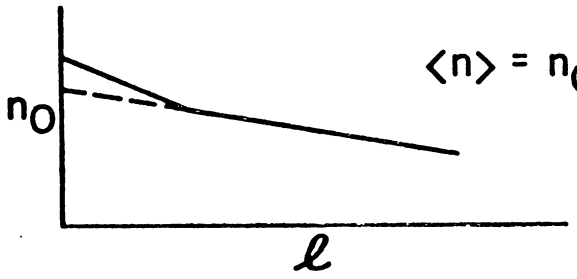

SCINTILLATOR		CLADDING	ℓ_0	$\langle n \rangle$ AT $\ell = 50$ cm
a	NE 110	None	30	$\ll 1$
b	NE 110	UV - Cured	80	2.6
c	NE 110	Silicone	100	4.5
d	NE 161	Silicone or Glass Resin (Composite curve, many trials)	115	4 - 4.8
e	NE 161	Glass and UV Buffer	115	4.0

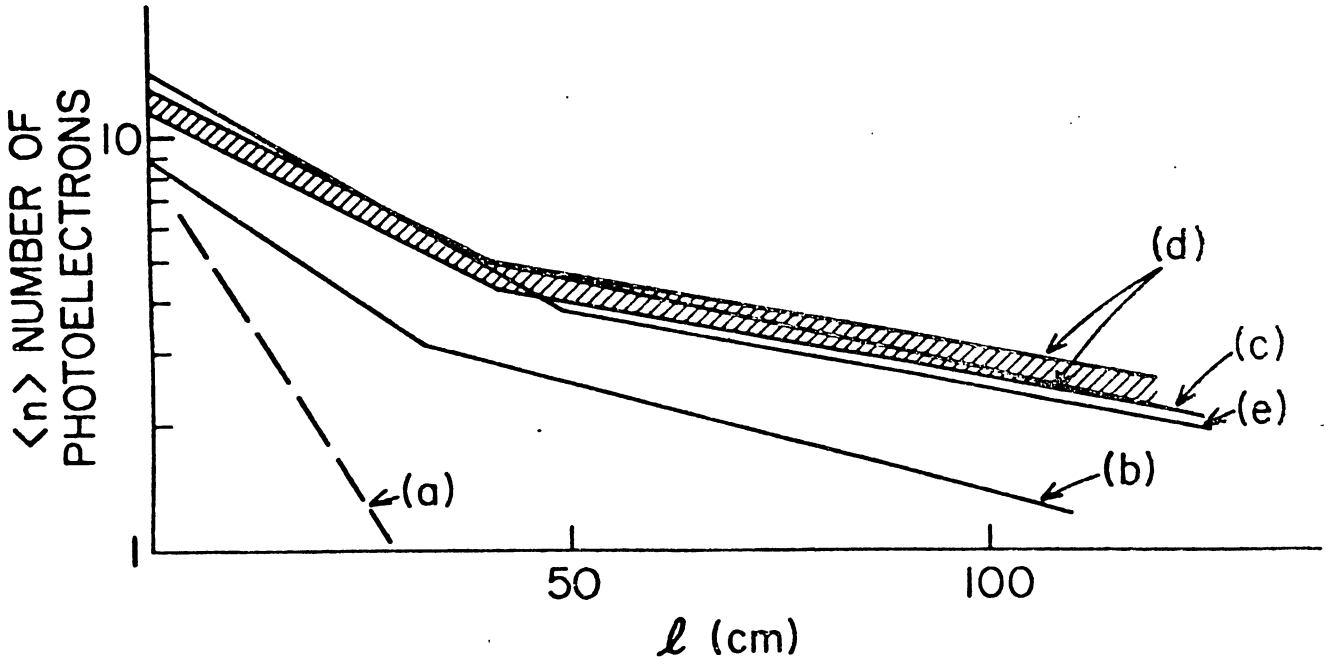

Fig. 10

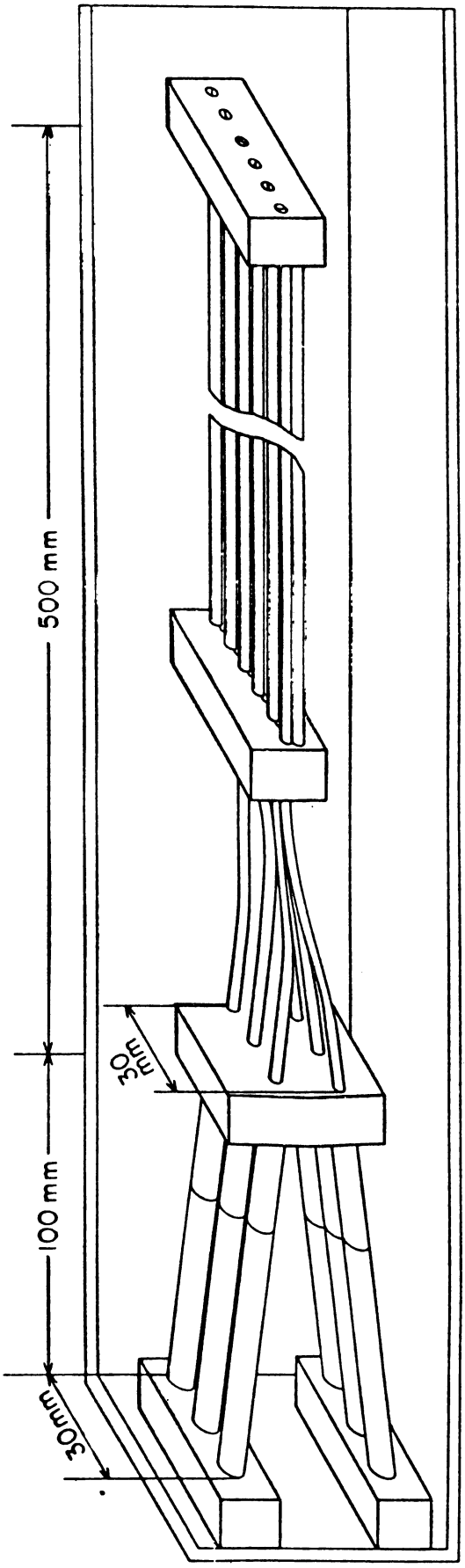

Fig. 11

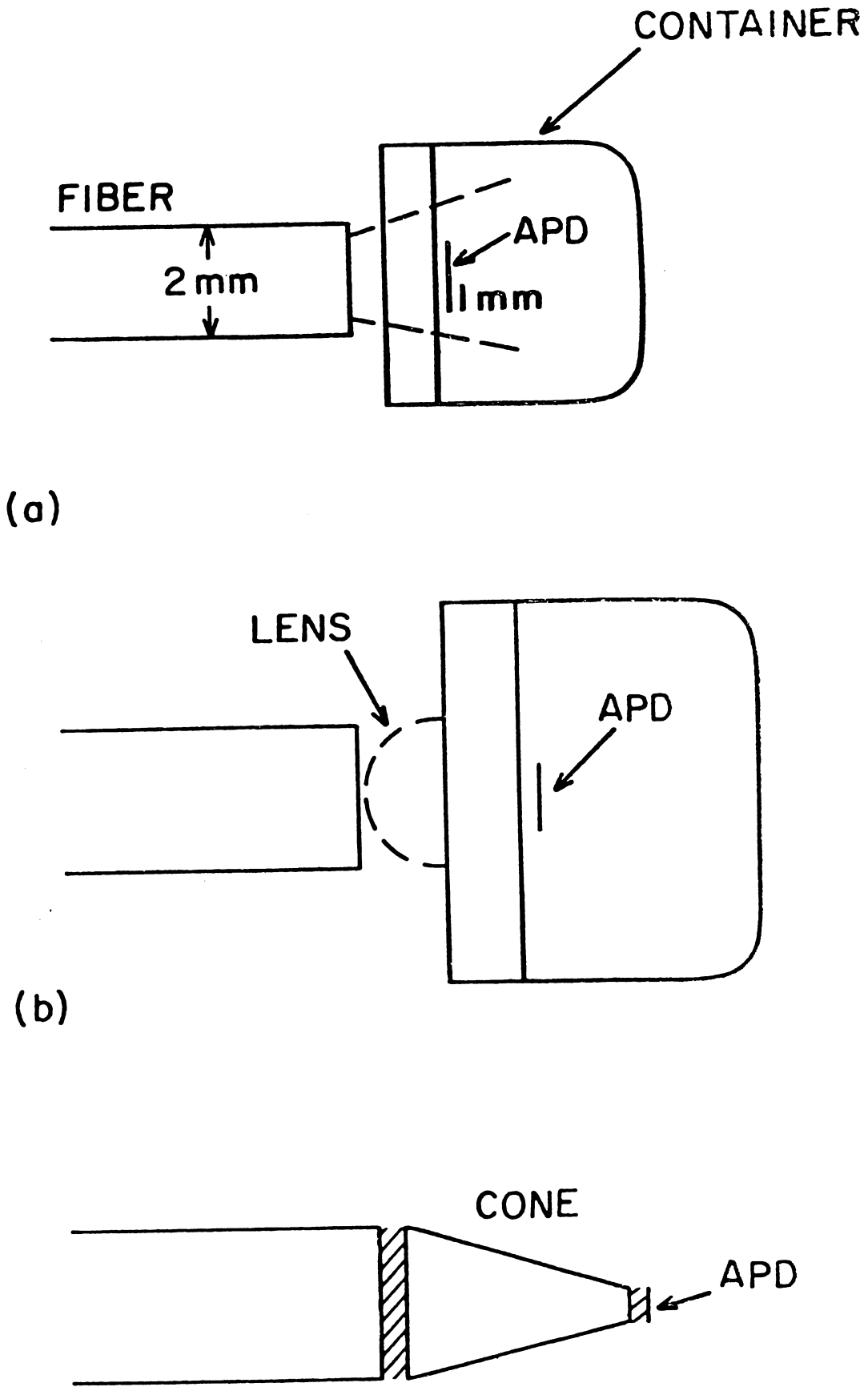

Fig. 12

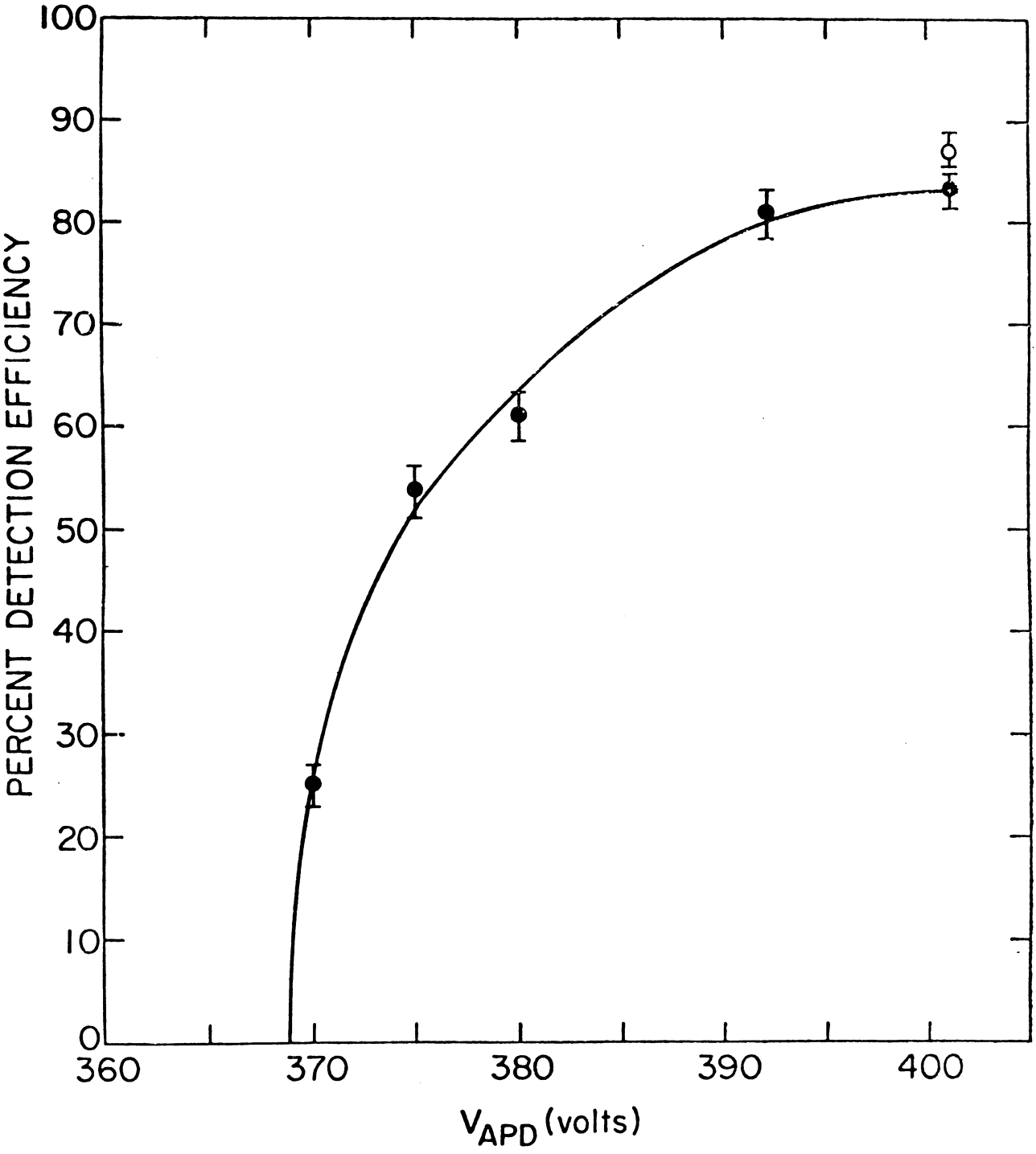
100
90
80
70
60
50
40
30
20
10
0
PERCENT DETECTION EFFICIENCY
360
370
380
390
400
V_{APD} (volts)

Fig. 13